Asia Pac. J. Math. 2025 **12**:42

MATHEMATICAL ANALYSIS OF FMD WITH OPTIMAL CONTROL

A.S. EEGUNJOBI*, N. CHERE, D. IIYAMBO, P.M. NDEEVELO

Mathematics Department, Namibia University of Science and Technology, Windhoek, Namibia

*Corresponding author: samdet1@yahoo.com

Received Mar. 8, 2025

Abstract. Foot-and-Mouth Disease (FMD) is a highly contagious infection that impacts livestock and poses significant economic challenges in Namibia. This study develops an $SEIRV$ mathematical model incorporating environmental transmission dynamics to analyze FMD spread. The model divides the population into Susceptible, Exposed, Infectious, Recovered, and Environmental compartments, accounting for pathogen shedding and decay. We derive the basic reproduction number R_0, conduct sensitivity analysis, and propose optimal control strategies using Pontryagin's principle. Simulations based on Namibian data highlight the need for integrated control measures, including environmental management and vaccination, to reduce FMD transmission.

2020 Mathematics Subject Classification. 92D30.

Key words and phrases. foot and mouth disease; optimal control; sensitivity, equilibrium analysis; positivity and boundlessness; environmental transmission; infection dynamics.

1. Introduction

Mathematical analysis serves as a fundamental tool for understanding complex real-world systems in various domains, including physical, economic, and biological sciences. It provides a rigorous framework through the theories of differentiation, integration, limits, and analytic functions, enabling the study of dynamic and intricate systems [12–14]. Among its numerous applications, mathematical modelling plays a crucial role in epidemiology, aiding in the prediction, control, and mitigation of infectious diseases.

In this study, we apply mathematical analysis to investigate the transmission dynamics of Foot-and-Mouth Disease (FMD), a highly contagious viral infection affecting livestock in Namibia. FMD has severe economic consequences, disrupting local and international trade in animal-based products [8]. Epidemiological modelling provides a structured approach to understanding the spread of such diseases, facilitating the design of effective control strategies. Our approach builds on classical

DOI: 10.28924/APJM/12-42

compartmental models, particularly the Susceptible-Infectious-Recovered (SIR) model, introduced by Kermack and McKendrick in the early 20th century [5].

Mathematical models have been widely employed in epidemiology to study disease dynamics and design intervention strategies. One of the earliest applications of mathematical modelling in disease control dates back to Bernoulli's analysis of smallpox vaccination in the 18th century [1]. Later, Ross developed mathematical frameworks for malaria prevention [2], while Eegunjobi et al. [3] studied the super-infection of two strains of the dengue virus, demonstrating how co-infection dynamics influence disease progression and control strategies. Van den Driessche and Watmough refined compartmental models to incorporate reproduction numbers and equilibrium analysis [4].

Recent studies have applied mathematical models to livestock diseases, including FMD. Zhao et al. [6] analyzed the economic impact of FMD outbreaks in the United States, emphasizing the importance of preventive measures. Coburn et al. [5] developed influenza transmission models, demonstrating the applicability of compartmental frameworks to various infectious diseases. Gaff and Schaefer [7] explored optimal vaccination and treatment strategies through mathematical optimization techniques.

Further advancements in epidemiological modelling involve extending the classical SIR model to incorporate additional compartments and demographic factors such as birth and death rates [9]. These extensions improve model accuracy and provide deeper insights into disease persistence and eradication strategies. Monteiro et al. [10] highlighted the role of incubation delays in shaping epidemic trends, while Song and Chen [11] examined optimal control strategies in structured populations.

Our study extends these theoretical foundations by formulating an FMD transmission model tailored to Namibia's livestock industry. We analyze the stability properties of equilibrium points, emphasizing the role of the basic reproduction number (R_0) in determining disease persistence or eradication. If $R_0 \leq 1$, the disease-free equilibrium is globally asymptotically stable, while for $R_0 > 1$, an endemic equilibrium emerges.

This study applies mathematical modelling to analyze FMD dynamics in Namibia, building upon classical and modern epidemiological frameworks. By incorporating demographic and control factors, our model offers insights into disease control strategies and long-term epidemic behavior.

The remaining sections of this article are arranged as follows: In section 2, we present the derivation of our model. Section 3 illustrates the main results, while Section 4 provides the application of the results to the formulated model with infection force under intervention policy to support our findings. In the last section, we provide a brief discussion and summary of the results.

2. Mathematical Formulation

We define the following compartments and transitions in the model: S: Susceptible individuals E: Exposed individuals I: Infectious individuals R: Recovered individuals $\mathcal{V}$: Environment (reservoir).

Susceptible (S) individuals enter the system at rate α, they can be infected by infectious individuals (βSI) or by exposure from the environment $(\lambda \mathcal{V} S)$. - Susceptible individuals die naturally at rate ϵ. In Exposed (E), Susceptible individuals move to the exposed compartment either due to infection by infectious individuals (βSI) or by exposure from the environment $(\lambda \mathcal{V} S)$. Exposed individuals transition to the infectious compartment at rate γE. Exposed individuals shed the virus back into the environment at rate ωE. Exposed individuals die naturally or from the disease at rate ϵ. In Infectious (I), Exposed individuals move to the infectious state at rate γE. Infectious individuals recover at rate θI or die at combined rate $\mu + \epsilon$. Infectious individuals shed the virus into the environment at rate ρI. Recovered (R) individuals return to immunity at rate θI and die naturally at rate ϵ.The Environment $(\mathcal{V})$ receives the virus from both exposed individuals (ωE) and infectious individuals (ρI). The environment decays naturally at rate δ, and contributes to new infections at rate $\lambda \mathcal{V} S$.

The corresponding differential equations for each compartment are given below:

$$\begin{aligned}
\frac{dS}{dt} &= \alpha - \beta SI - \lambda \mathcal{V} S - \epsilon S, \\
\frac{dE}{dt} &= \beta SI + \lambda \mathcal{V} S - (\gamma + \epsilon) E - \omega E, \\
\frac{dI}{dt} &= \gamma E - (\mu + \epsilon + \theta) I - \rho I, \\
\frac{dR}{dt} &= \theta I - \epsilon R, \\
\frac{d\mathcal{V}}{dt} &= \rho I + \omega E - \lambda \mathcal{V} - \delta \mathcal{V}
\end{aligned} \tag{1}$$

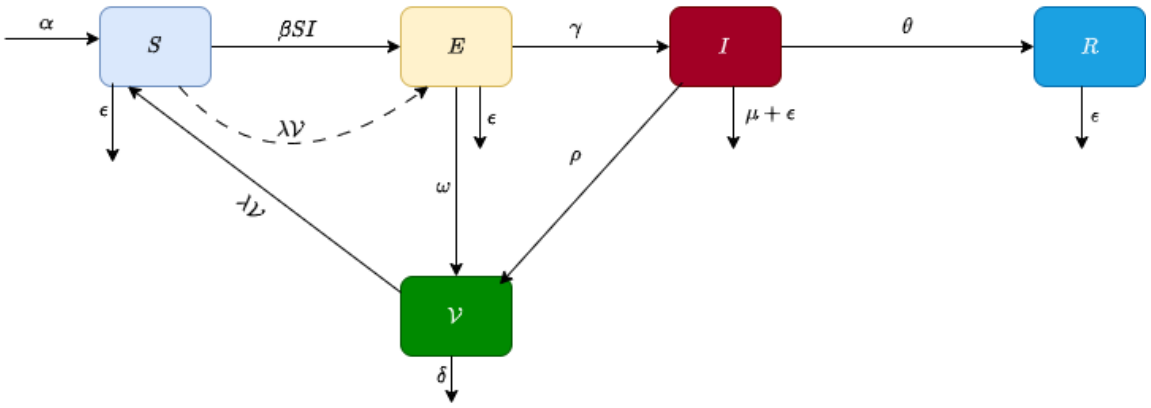

FIGURE 1. Diagram

3. MATHEMATICAL ANALYSIS OF THE $SEIR\mathcal{V}$ MODEL

Initially, the study assesses the well-posedness of the model by investigating the positivity and boundedness of the solutions for S, E, I, and R in relation to time (t). These analytical assessments are pivotal in establishing the biological significance of the formulated environmental FMD model.

3.1. **Positive Invariance of the $SEIR\mathcal{V}$ Model.** To ensure the model is biologically meaningful, we define the feasible region:

$$\Omega = \left\{(S, E, I, R, \mathcal{V}) \in \mathbb{R}^5_+ \mid S + E + I + R = N, \quad S, E, I, R \geq 0, \quad \mathcal{V} \geq 0\right\}.$$

Considering

$$\frac{dS}{dt} = \alpha - \beta SI - \lambda \mathcal{V} S - \epsilon S \implies \frac{dS}{dt} + Sp(t) = \alpha \quad \text{where} \quad p(t) = \beta I + \lambda \mathcal{V} + \epsilon$$

solving, we obtain

$$S(t) = S(0) + e^{-\int \beta I + \lambda \mathcal{V} + \epsilon dn} \Big[\int_0^t \alpha e^{-\int \beta I + \lambda \mathcal{V} + \epsilon dn} dt \Big] \geq 0. \tag{2}$$

$\forall t \geq 0, S(t) \geq 0$, this is also true for $E(t) \geq 0, I(t) \geq 0, R(t) \geq 0$, and $\mathcal{V} \geq 0$.

3.2. **Boundedness of Solutions for the $SEIR$ Model.** Since $S + E + I + R = N$, we already know that S, E, I, R are bounded. We now check the boundedness of $\mathcal{V}$.

Solving:

$$\mathcal{V}(t) = e^{-(\lambda+\delta)t} \Big[\mathcal{V}(0) + \int_0^t (\rho I + \omega E) e^{(\lambda+\delta)t} dt \Big]. \tag{3}$$

Since $I(t)$ is bounded, the integral remains finite, ensuring that $\mathcal{V}$ is bounded.

Since all state variables remain non-negative and bounded, we conclude that the feasible region Ω is positively invariant under the system dynamics. This ensures that the model remains biologically meaningful for all $t \geq 0$

3.3. **Disease-free and endemic Equilibrium.** The disease free equilibrium is given as

$$(S, E, I, R, \mathcal{V}) = (\frac{\alpha}{\epsilon}, 0, 0, 0, 0)$$

The endemic equilibrium is given by:

$$S^* = \frac{(\gamma + \epsilon + \omega)(\mu + \epsilon + \theta + \rho)(\lambda + \delta)}{\beta\gamma(\lambda + \delta) + \lambda\left(\omega(\mu + \epsilon + \theta + \rho) + \rho\gamma\right)},$$

$$E^* = (\mu + \epsilon + \theta + \rho)\frac{I^*}{\gamma},$$

$$I^* = \frac{\alpha\gamma(\gamma + \epsilon + \omega)(\mu + \epsilon + \theta + \rho) - \epsilon(\lambda + \delta)}{\beta\gamma(\lambda + \delta) + \lambda\left(\omega(\mu + \epsilon + \theta + \rho) + \rho\gamma\right)},$$

$$R^* = \frac{\theta}{\epsilon} I^*,$$

$$V^* = \frac{\omega(\mu + \epsilon + \theta + \rho) + \rho\gamma}{\gamma(\lambda + \delta)} I^*.$$

3.4. **The Basic Reproduction Number R_0.** Building on the approach presented in [4]- [15] and leveraging the next-generation matrix method, we proceed to compute the basic reproduction number through a structured sequence of steps. Considering the right hand side of equation $E(t), I(t)$ and $\mathcal{V}$ in equation (1) we derive $\mathcal{F} - \mathcal{U}$, where $\mathcal{F}$ represents new infections, while $\mathcal{U}$ accounts for all other terms governing the dynamics of the compartment under consideration. The new infections from $E, I, \mathcal{V}$ is given as

$\mathcal{F} = \begin{bmatrix} (\beta SI + \lambda \mathcal{V} S \\ 0 \\ 0 \end{bmatrix}$. At the disease-free equilibrium (DFE), we where $S = \frac{\alpha}{\epsilon}$ and $E = I = \mathcal{V} = 0$, so the Jacobian of F with respect to $(E, I, \mathcal{V})$ is:

$F = \begin{bmatrix} 0 & \frac{\beta\alpha}{\epsilon} & \frac{\lambda\alpha}{\epsilon} \\ 0 & 0 & 0 \\ 0 & 0 & 0 \end{bmatrix}$. From the equations of $E, I, \mathcal{V}$, the transition terms are:

$V = \begin{bmatrix} (\gamma + \epsilon + \omega)E \\ -\gamma E + (\mu + \epsilon + \theta + \rho)I \\ -\omega E - \rho I + (\lambda + \delta)\mathcal{V} \end{bmatrix}$. Taking the Jacobian of V with respect to $(E, I, \mathcal{V})$, we get:

$V = \begin{bmatrix} \gamma + \epsilon + \omega & 0 & 0 \\ -\gamma & \mu + \epsilon + \theta + \rho & 0 \\ -\omega & -\rho & \lambda + \delta \end{bmatrix}$ and

$$V^{-1} = \begin{bmatrix} \frac{1}{\gamma+\epsilon+\omega} & 0 & 0 \\ \frac{\gamma}{(\gamma+\epsilon+\omega)(\mu+\epsilon+\theta+\rho)} & \frac{1}{\mu+\epsilon+\theta+\rho} & 0 \\ \frac{\omega\epsilon+\gamma\rho+\omega\mu+\omega\rho+\omega\theta}{(\gamma+\epsilon+\omega)(\mu+\epsilon+\theta+\rho)(\lambda+\delta)} & \frac{\rho}{(\mu+\epsilon+\theta+\rho)(\lambda+\delta)} & \frac{1}{\lambda+\delta} \end{bmatrix}.$$

We compute the FV^{-1} and the basic reproduction number R_0 for the problem under consideration is defined as the spectral radius of the non-negative matrix FV^{-1}, denoted mathematically as $R_0 = \rho(FV^{-1})$.

$$R_0 = \frac{\beta\,\alpha\,\gamma}{\epsilon\,(\gamma+\epsilon+\omega)\,(\mu+\epsilon+\theta+\rho)} + \frac{\alpha\,\gamma\,\lambda\,\rho}{\epsilon\,(\gamma+\epsilon+\omega)\,(\mu+\epsilon+\theta+\rho)\,(\lambda+\delta)} + \frac{\alpha\,\lambda\,\omega}{(\gamma+\epsilon+\omega)\,(\lambda+\delta)\,\epsilon} \tag{4}$$

The basic reproduction number, R_0, is defined as the average number of secondary infections produced by one infectious individual in a completely susceptible population. This term represents the average number of new infections generated through direct contact with an infectious FMD animal. When an infectious animal sheds the virus, the overall chance that this environmental virus leads to a new infection is captured by second term in the R_0 expression. This term quantifies the new infections generated indirectly via the environment contaminated by infectious animals while the third term

captures the infections due to environmental contamination that originate from animals that are still in the incubation phase. This is indirect transmission via the environment from exposed animals.

Sensitivity Analysis of R_0

The normalized sensitivity indices $\Gamma_{\psi}^{R_0}$ as in [22] quantify the proportional change in R_0 due to a small change in parameter ψ defined as

$$\Gamma_{\psi}^{R_0} = \frac{\partial R_0}{\partial \psi} \times \frac{\psi}{R_0}. \tag{5}$$

Positive values indicate R_0 increases with ψ, while negative values indicate R_0 decreases with ψ. The magnitude reflects the strength of the effect. The normalized sensitivity indices for each parameter is given as

$$\Gamma_{\alpha}^{R_0} > 0, \Gamma_{\beta}^{R_0} > 0, \Gamma_{\lambda}^{R_0} > 0, \Gamma_{\gamma}^{R_0} > 0$$

while

$$\Gamma_{\epsilon}^{R_0} < 0, \Gamma_{\omega}^{R_0} < 0, \Gamma_{\mu}^{R_0} < 0, \Gamma_{\theta}^{R_0} < 0, \Gamma_{\rho}^{R_0} < 0, \Gamma_{\delta}^{R_0} < 0,$$

and illustrated in Fig.

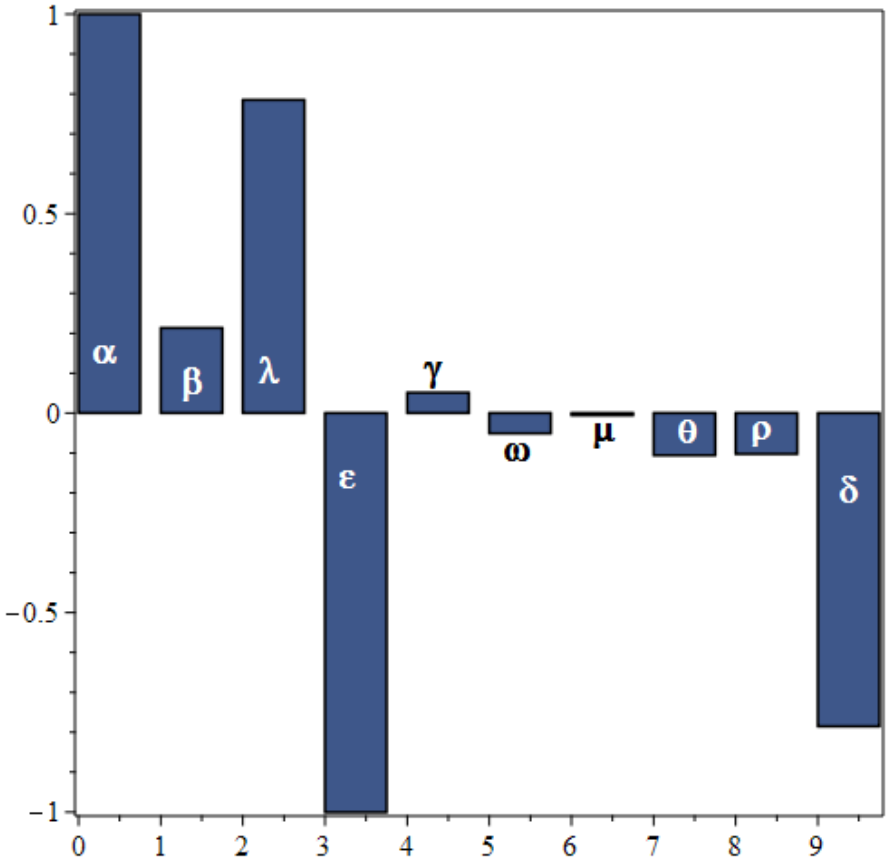

Figure 2. Sensitivity indices graph

TABLE 1. Normalized Sensitivity Indices of R_0

Parameter (K)	Sensitivity Index ($\Gamma_K^{R_0}$)	Interpretation
α (Recruitment rate)	1.000	Strongest positive effect.
β (Direct transmission rate)	0.213	Moderate positive effect.
λ (Environmental transmission rate)	0.785	Large positive effect.
ϵ (Natural death rate)	-1.001	Strongest negative effect.
γ (Transition rate: $E \to I$)	0.051	Weak positive effect.
ω (Shedding rate: $E \to \mathcal{V}$)	-0.051	Weak negative effect.
μ (Disease-induced death rate)	-0.005	Negligible negative effect.
θ (Recovery rate)	-0.106	Moderate negative effect.
ρ (Shedding rate: $I \to \mathcal{V}$)	-0.102	Weak negative effect.
δ (Environment decay rate)	-0.785	Large negative effect.

It is observed form the estimation that α and λ are the strongest positive drivers of R_0 while ϵ and δ are the strongest negative drivers.Reducing environmental transmission (λ) and enhancing pathogen decay (δ) are critical for controlling R_0. Counterintuitively, higher shedding rates (ω, ρ) slightly reduce R_0, suggesting complex interactions in the model. This investigation highlights the importance of environmental transmission (λ) and decay (δ) in FMD disease spread. Public health strategies should prioritize reducing environmental contamination and enhancing pathogen degradation.

4. Optimal Control

In this section, we analyse the optimality function of $SEIR\mathcal{V}$ model using control variables u_1 and u_2. The system dynamics with controls u_1, and u_u is given by:

$$\begin{aligned}
\frac{dS}{dt} &= \alpha - \beta SI - \lambda \mathcal{V} S - (\epsilon + u_1)S, \\
\frac{dE}{dt} &= \beta SI + \lambda \mathcal{V} S - (\gamma + \epsilon + \omega)E, \\
\frac{dI}{dt} &= \gamma E - (\mu + \epsilon + \theta + \rho)I, \\
\frac{dR}{dt} &= \theta I - \epsilon R + u_1 S \\
\frac{d\mathcal{V}}{dt} &= \rho I + \omega E - (\lambda + \delta + u_2)\mathcal{V}
\end{aligned} \tag{6}$$

Our mail goal is to reduce the number of infections and minimize environmental contamination. We minimize the number of infections while controlling intervention costs:

$$J(u_1, u_2) = \int_0^T \left[AE(t) + BI(t) + C\mathcal{V}(t) + \frac{D_1}{2}u_1^2(t) + \frac{D_2}{2}u_2^2(t) \right] dt, \tag{7}$$

where A, B, C penalize FMD burden, and D_1, D_2 are positive weight control costs. We adopt the Pontryagin's maximum principle to find the optimal solution for the model.

Apply the Hamiltonian H to obtain the minimum value of Pontryagin's maximum principle, which is given

$$\begin{aligned} H = {} & AE + BI + C\mathcal{V} + \frac{D_1}{2}u_1^2 + \frac{D_2}{2}u_2^2 + \lambda_S\left[\alpha - \beta SI - \lambda\mathcal{V}S - (\epsilon + u_1)S\right] \\ & + \lambda_E\left[\beta SI + \lambda\mathcal{V}S - (\gamma + \epsilon + \omega)E\right] + \lambda_I\left[\gamma E - (\mu + \epsilon + \theta + \rho)I\right] \\ & + \lambda_R\left[\theta I - \epsilon R + u_1 S\right] + \lambda_{\mathcal{V}}\left[\rho I + \omega E - (\lambda + \delta + u_2)\mathcal{V}\right] \end{aligned} \tag{8}$$

Theorem 4.1. There exists an optimal control u_1^*, u_2^* and the corresponding solution $(S^*, E^*, I^*, R^*\mathcal{V}^*)$ that minimizes J. For the above statement to be true, there exists adjoint functions $\lambda_S(t), \lambda_E(t), \lambda_I(t), \lambda_R(t), \lambda_{\mathcal{V}}(t)$ such that

$$\begin{aligned} \frac{d\lambda_S}{dt} &= (\beta I + \lambda\mathcal{V} + \epsilon + u_1)\lambda_S - (\beta I + \lambda\mathcal{V})\lambda_E - u_1\lambda_R \\ \frac{d\lambda_E}{dt} &= -A + (\gamma + \epsilon + \omega)\lambda_E - \gamma\lambda_I - \omega\lambda_{\mathcal{V}} \\ \frac{d\lambda_I}{dt} &= -B + \beta S(\lambda_S - \lambda_E) + (\mu + \epsilon + \theta + \rho)\lambda_I - \theta\lambda_R - \rho\lambda_{\mathcal{V}} \\ \frac{d\lambda_R}{dt} &= \epsilon\lambda_R \\ \frac{d\lambda_{\mathcal{V}}}{dt} &= -C + \lambda S(\lambda_S - \lambda_E) + (\lambda + \delta + u_2)\lambda_{\mathcal{V}} \end{aligned} \tag{9}$$

with the transversality conditions

$$\lambda_S(T) = \lambda_E(T) = \lambda_I(T) = \lambda_R(T) = \lambda_{\mathcal{V}}(T) = 0.$$

Also,

$$\begin{aligned} u_1^* &= \max\left(0, \min\left(u_1^{max}, \frac{(\lambda_S - \lambda_R)S}{D_1}\right)\right), \\ u_2^* &= \max\left(0, \min\left(u_2^{max}, \frac{\lambda_{\mathcal{V}}\mathcal{V}}{D_2}\right)\right). \end{aligned} \tag{10}$$

Proof. To find the optimal controls u_1^* and u_2^*, we use the Pontryagin Maximum Principle, which requires that the optimal controls maximize the Hamiltonian. The partial derivatives of H with respect to u_1 and u_2 are:

$$\frac{\partial H}{\partial u_1} = D_1 u_1 - \lambda_S S + \lambda_R S, \qquad \frac{\partial H}{\partial u_2} = D_2 u_2 - \lambda_{\mathcal{V}}\mathcal{V}.$$

Setting these derivatives to zero for optimality:

$$D_1 u_1 - (\lambda_S - \lambda_R)S = 0, \qquad D_2 u_2 - \lambda_{\mathcal{V}}\mathcal{V} = 0.$$

Solving for u_1 and u_2:

$$u_1 = \frac{(\lambda_S - \lambda_R)S}{D_1}, \qquad u_2 = \frac{\lambda_{\mathcal{V}}\mathcal{V}}{D_2}.$$

Since the controls are constrained by $0 \leq u_1 \leq u_1^{max}$ and $0 \leq u_2 \leq u_2^{max}$, we apply the projection condition:

$$u_1^* = \max\left(0, \min\left(u_1^{max}, \frac{(\lambda_S - \lambda_R)S}{D_1}\right)\right), \qquad u_2^* = \max\left(0, \min\left(u_2^{max}, \frac{\lambda_{\mathcal{V}}\mathcal{V}}{D_2}\right)\right).$$

□

u_1^* represents the optimal level of intervention that reduces the susceptible population S moving into infected states. The expression ensures that the control remains within feasible bounds, avoiding negative or excessive values. u_2^* represents the optimal level of environmental control effort applied to reduce the presence of Foot and Mouth Disease (FMD) in the environment. This could include disinfection of contaminated areas, movement restrictions, or biosecurity measures. Again, it ensures that the control is within the allowed range

4.1. **Numerical Simulation Results.** By applying the data presented in Table 3 to our $SEIR\mathcal{V}$ model, we calculated a basic reproduction number of $R_0 = 2$.. Since $R_0 > 1$, this indicates that the foot-and-mouth disease (FMD) is expected to spread through the population, potentially triggering an outbreak.

Figure 2 further illustrates how the $SEIR\mathcal{V}$ model uses the specified variables and parameter values to simulate the disease dynamics over time. Notably, the figure shows an encouraging trend: by day 20, the infection rate falls to zero. This decline suggests that despite the initial potential for rapid disease transmission, the progression of the outbreak may be effectively controlled as the infection subsides over time. Additionally, the FMD recovery curve displays a markedly steep incline early in the outbreak, indicating that infected livestock are recovering at an accelerated rate. This trend suggests that improvements in veterinary care, may be significantly boosting recovery rates. As these advancements take effect, they likely contribute to reducing the overall impact of the FMD outbreak by shortening the infectious period and limiting further transmission.

Moreover, the curve representing exposed livestock exhibits a clear downward trend, declining steadily over time and reaching zero at approximately 24 days. This rapid decrease suggests that the latent period during which livestock are susceptible but not yet infectious is relatively short, or that early intervention measures (such as prompt detection, quarantine, and vaccination) are highly effective in preventing further exposures. The reduction of exposed livestock to zero is a promising sign, as it implies that new cases are no longer emerging in this category, thereby helping to contain the outbreak. Additionally, the model reveals that the environmental factor follows an intriguing pattern during the outbreak. Initially, this factor increases as the virus accumulates in the environment—likely due to early shedding from infected animals and the lack of immediate decontamination. However, after approximately 20 days, the environmental factor begins to decline. This downturn may be

attributed to effective decontamination measures, the natural decay of the virus, or adaptive changes in environmental conditions that reduce viral persistence.

An increase in the infectious rate expedites disease progression, significantly impacting the dynamics of the exposed compartment. As this rate rises, livestock quickly transition from the exposed state to the infectious stage, resulting in a marked reduction in the number of animals remaining in the exposed compartment, as illustrated in Fig. 4. Concurrently, this rapid progression leads to an expanded recovery compartment, with more animals moving through the stages of infection and eventually recuperating.

As the rates ω and ρ increase, as shown in Fig.5, the amount of virus shed by these groups rises, leading to a significant accumulation of the pathogen in the environment. This elevated viral presence not only reflects the intensity of the outbreak but also enhances the potential for secondary infections, as the FMD virus can persist in environmental reservoirs. The figure clearly demonstrates that higher values ofω and ρ are directly associated with an increase in $\mathcal{V}$ underscoring the importance of controlling virus shedding to mitigate the spread of FMD. Fig.6 illustrate the impact of $gamma$ on the recovery compartment. Increasing γ shortens the time spent in the exposed compartment, leading to a faster accumulation of animals in the infectious compartment.This in turn feeds the recovery process, as more infectious animals translate into more recovered compartment. The rate of increase in R depends on both γ, meaning that if γ increases, R increases proportionally.

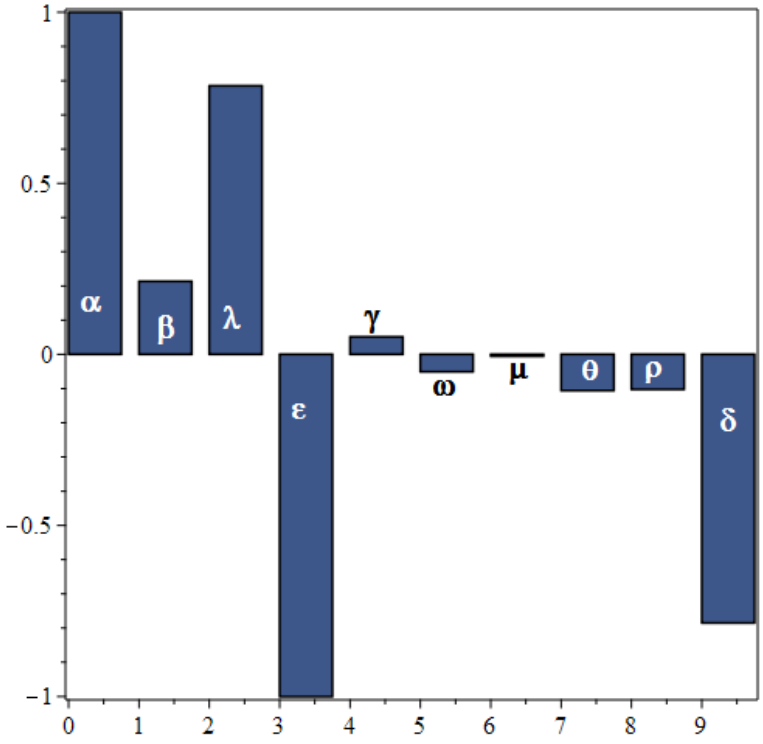

FIGURE 3. Sensitivity indices graph

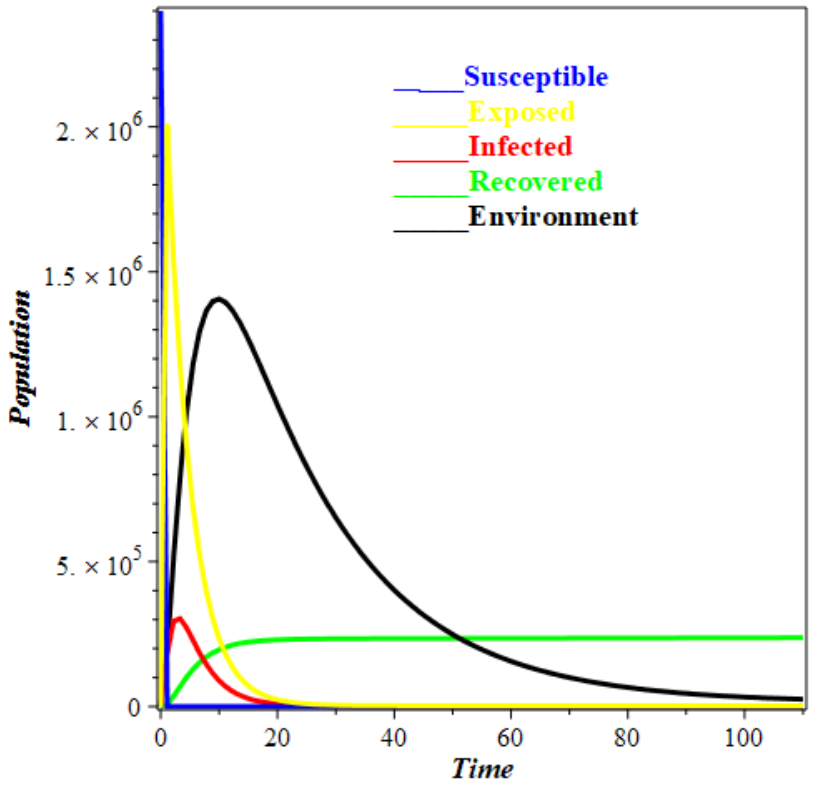

Fig.3: Trends in Population Change

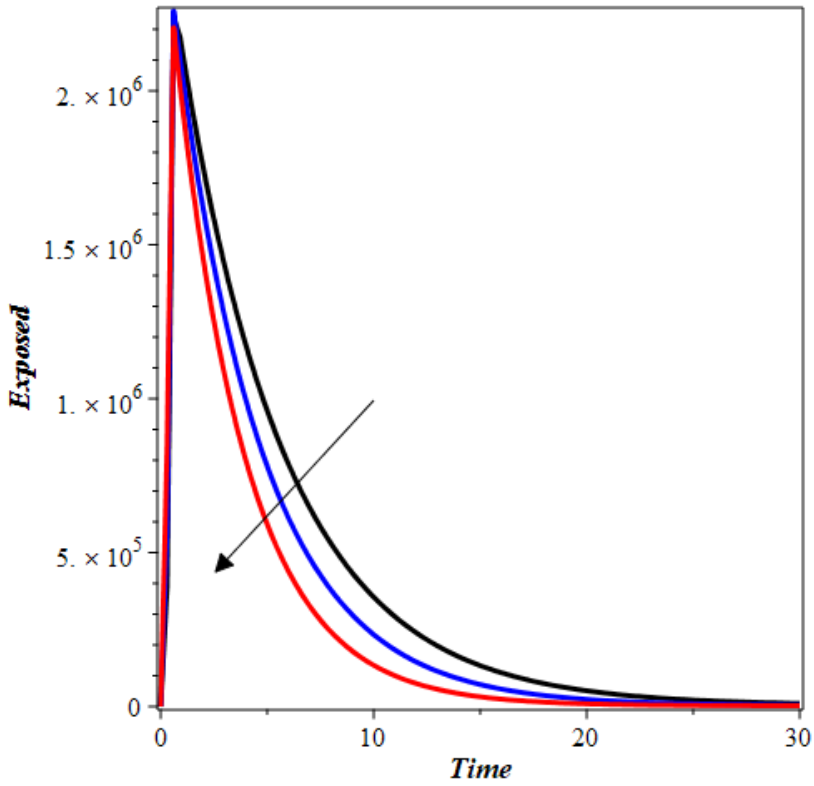

Fig.4: Impact of increasing γ on exposed

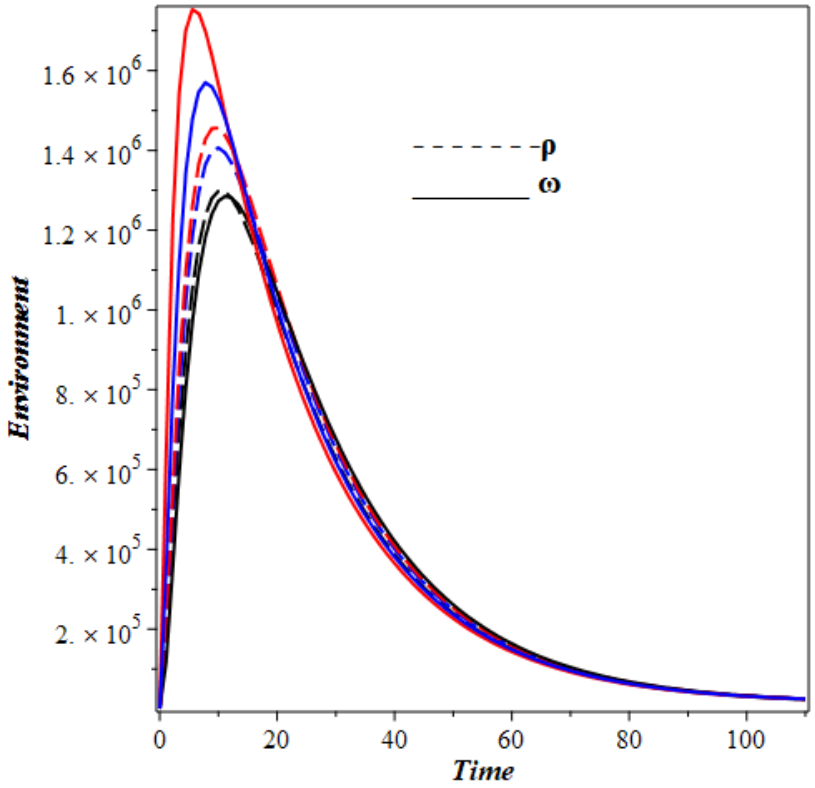

Fig.5: Impact of ω and ρ on environment

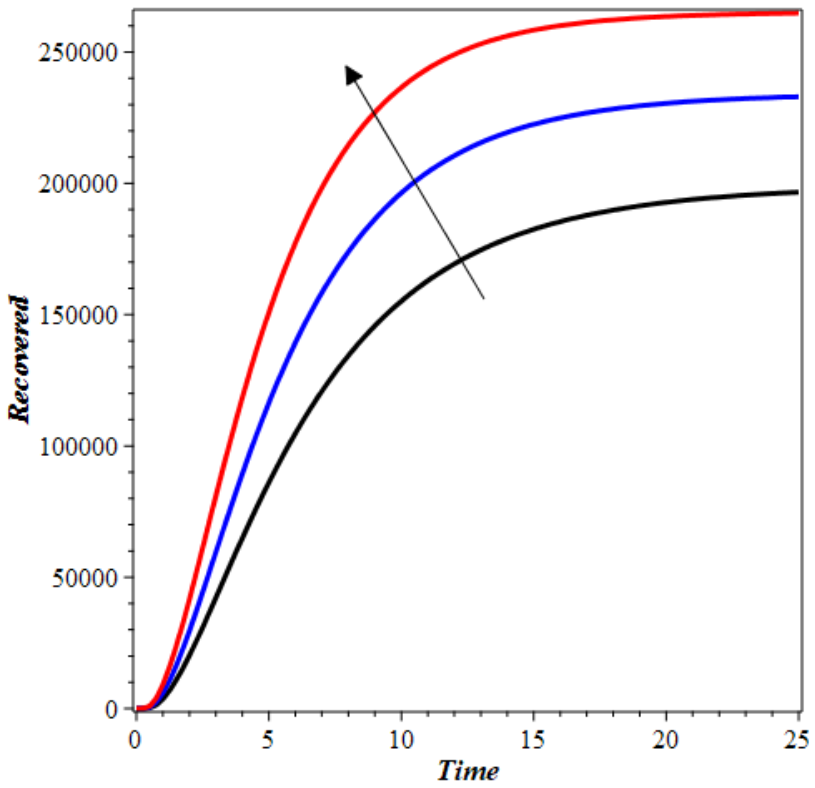

Fig.5: Impact of increasing γ on recovery

TABLE 2. Initial Conditions (Variables)

Variable	Value	Reference
S(0)	2.4×10^6	[23]
$E(0)$	100	[26]
$I(0)$	50	[24]
$R(0)$	0	Assumed
$\mathcal{V}(0)$	1,000	[27]

TABLE 3. Parameter Values

Parameter	Value	Unit	Description	Reference
α	750	individuals/day	Cattle birth rate	[23]
β	0.0005	individuals^{-1}·day^{-1}	Direct transmission rate	[24]
λ	0.0001	(TCID$_{50}$/mL)$^{-1}$·day^{-1}	Environmental transmission rate	[25]
ϵ	0.00014	day^{-1}	Natural mortality rate	[23]
γ	0.1429	day^{-1}	Progression rate (latent to infectious)	[27]
ω	0.1	TCID$_{50}$·individual^{-1}·day^{-1}	Shedding rate (exposed)	[26]
μ	0.005	day^{-1}	Disease-induced mortality rate	[24]
θ	0.1	day^{-1}	Recovery rate	[25]
ρ	0.5	TCID$_{50}$·individual^{-1}·day^{-1}	Shedding rate (infectious)	[26]
δ	0.05	day^{-1}	Environmental decay rate	[27]

5. Conclusion

This study develops a compartmental mathematical model to explore the transmission dynamics of foot-and-mouth disease, incorporating data from Namibia for numerical simulations and sensitivity analysis. The model's solutions were proven to be both positive and bounded. Furthermore, equilibrium points were identified, and optimal control strategies were examined. The basic reproduction number was derived, and extensive numerical simulations were performed. Our findings yield the following key insights:

- u_1^* and u_2^* expressions provide the optimal control strategies for minimizing the objective functional while satisfying the system dynamics.
- our investigation highlights the importance of environmental transmission (λ) and decay (δ) in disease spread. Public health strategies should prioritize reducing environmental contamination and enhancing pathogen degradation.
- Increasing γ reduces the susceptible population while expanding the recovered compartment.

- An increase in both ρ and ω initially amplifies the environmental compartment before causing its decline.

Conflicts of Interest. The authors declare that there are no conflicts of interest regarding the publication of this paper.

References

[1] D. Bernoulli, Essai d'une Nouvelle Analyse de la Mortalité Causée par la Petite Vérole, Mém. Math. Phys. Acad. Roy. Sci., Paris (1766), 1–45.

[2] R. Ross, The Prevention of Malaria, Murray, London, 1911.

[3] A.S. Eegunjobi, M.C. Anyanwu, S.N. Neossi-Nguetchue, Modelling the Super-Infection of Two Strains of Dengue Virus, J. Egypt. Math. Soc. 31 (2023), 1. https://doi.org/10.1186/s42787-023-00161-6.

[4] P. Van Den Driessche, J. Watmough, Reproduction Numbers and Sub-Threshold Endemic Equilibria for Compartmental Models of Disease Transmission, Math. Biosci. 180 (2002), 29–48. https://doi.org/10.1016/S0025-5564(02)00108-6.

[5] B.J. Coburn, B.G. Wagner, S. Blower, Modeling Influenza Epidemics and Pandemics: Insights into the Future of Swine Flu (H1N1), BMC Med. 7 (2009), 30. https://doi.org/10.1186/1741-7015-7-30.

[6] Z. Zhao, T.I. Wahl, T.L. Marsh, Invasive Species Management: Foot-and-Mouth Disease in the U.S. Beef Industry, Agric. Resour. Econ. Rev. 35 (2006), 98–115. https://doi.org/10.1017/S106828050001008X.

[7] H. Gaff, E. Schaefer, Optimal Control Applied to Vaccination and Treatmentstrategies for Various Epidemiological Models, Math. Biosci. Eng. 6 (2009), 469–492. https://doi.org/10.3934/mbe.2009.6.469.

[8] World Organisation for Animal Health, Foot and Mouth Disease, https://www.woah.org/en/disease/foot-and-mouth-disease.

[9] Md. Samsuzzoha, A Study on Numerical Solutions of Epidemic Models, Thesis, Swinburne University of Technology, Australia, 2012.

[10] L.H.A. Monteiro, J.B. Sasso, J.G. Chaui Berlinck, Continuous and Discrete Approaches to the Epidemiology of Viral Spreading in Populations Taking into Account the Delay of Incubation Time, Ecol. Model. 201 (2007), 553–557. https://doi.org/10.1016/j.ecolmodel.2006.09.027.

[11] X. Song, L. Chen, Optimal Harvesting and Stability for a Two-Species Competitive System with Stage Structure, Math. Biosci. 170 (2001), 173–186. https://doi.org/10.1016/S0025-5564(00)00068-7.

[12] F. Brauer, Compartmental Models in Epidemiology, in: F. Brauer, P. Van Den Driessche, J. Wu (Eds.), Mathematical Epidemiology, Springer, Berlin, Heidelberg, 2008: pp. 19–79. https://doi.org/10.1007/978-3-540-78911-6_2.

[13] H.W. Hethcote, The Mathematics of Infectious Diseases, SIAM Rev. 42 (2000), 599–653. https://doi.org/10.1137/S0036144500371907.

[14] M.J. Keeling, P. Rohani, Modeling Infectious Diseases in Humans and Animals, Princeton University Press, 2008.

[15] O. Diekmann, J.A.P. Heesterbeek, M.G. Roberts, The Construction of Next-Generation Matrices for Compartmental Epidemic Models, J. R. Soc. Interface 7 (2010), 873–885. https://doi.org/10.1098/rsif.2009.0386.

[16] S.A. Al-Sheikh, Modeling and Analysis of an SEIR Epidemic Model with a Limited Resource for Treatment, Glob. J. Sci. Front. Res. Math. Decis. Sci. 12 (2012), 58–64.

[17] N. Khalil, Optimality Conditions for Optimal Control Problems and Applications, Thesis, Université de Bretagne Occidentale - Brest, (2017). https://theses.hal.science/tel-01740334v1.

[18] Ministry of Agriculture, Water, and Forestry of Namibia, Veterinary Databases, (2023).

[19] Food and Agriculture Organization of the United Nations, Central Veterinary Laboratory, https://www.fao.org/south-south-gateway/database/detail/en/c/414247.

[20] S. Mushayabasa, G. Tapedzesa, Modeling the Effects of Multiple Intervention Strategies on Controlling Foot-and-Mouth Disease, BioMed Res. Int. 2015 (2015), 584234. https://doi.org/10.1155/2015/584234.

[21] National Library of Medicine, Veterinary Science Search and Veterinary Information Resources, (2007). https://www.nlm.nih.gov/services/queries/veterinarymed.html.

[22] A.S. Eegunjobi, O.D. Makinde, Impact of Corruption in a Society With Exposed Honest Individuals: A Mathematical Model, Asia Pac. J. Math. 10 (2023), 18. https://doi.org/10.28924/APJM/10-18.

[23] Food and Agriculture Organization, The State of Food and Agriculture 2010-2011, https://www.fao.org/4/i2050e/i2050e00.htm.

[24] G.R. Thomson, W. Vosloo, A.D.S. Bastos, Foot and Mouth Disease in Wildlife, Virus Res. 91 (2003), 145–161. https://doi.org/10.1016/S0168-1702(02)00263-0.

[25] T.J.D. Knight-Jones, J. Rushton, The Economic Impacts of Foot and Mouth Disease – What Are They, How Big Are They and Where Do They Occur?, Prev. Vet. Med. 112 (2013), 161–173. https://doi.org/10.1016/j.prevetmed.2013.07.013.

[26] B. Molla, G. Ayelet, Y. Asfaw, Y. Jibril, G. Ganga, E. Gelaye, Epidemiological Study on Foot-and-Mouth Disease in Cattle: Seroprevalence and Risk Factor Assessment in South Omo Zone, South-Western Ethiopia: Epidemiological Study on Foot-and-Mouth Disease in Cattle, Transbound. Emerg. Dis. 57 (2010), 340–347. https://doi.org/10.1111/j.1865-1682.2010.01154.x.

[27] World Organisation for Animal Health, Terrestrial Code Online Access, https://www.woah.org/en/what-we-do/standards/codes-and-manuals/terrestrial-code-online-access/.